sciendo

ISSN 1335-8871

MEASUREMENT SCIENCE REVIEW

Journal homepage: https://content.sciendo.com

Comparison of Low-Cost GNSS Receivers for Time Transfer using Zero-Length Baseline

Marek Doršic

Faculty of Mechanical Engineering, Slovak University of Technology, Bratislava, Slovakia, marek.dorsic@gmail.com
Slovak Institute of Metrology, Bratislava, Slovakia

Abstract: A comparison between low-cost single-frequency and dual-frequency Global Navigation Satellite System (GNSS) receiver timing modules is presented, focusing on their suitability for time transfer applications. The study uses a zero-length baseline measurement approach to assess their performance and highlights the advantages of dual-frequency receivers. The clock comparison residuals between these low-cost devices and a reference receiver are analyzed. In particular, it is shown that the use of averages longer than 200 s can effectively mitigate the quantization error inherent in pulse per second outputs of the timing modules. The results showcase sub-nanosecond time deviation instabilities between the reference receiver and the dual-frequency timing module. In contrast, the single-frequency module exhibits time deviations of 3.3 ns at a one-day averaging interval. This research provides insights into the selection and utilization of GNSS timing modules for time transfer applications, where such modules can serve as attractive, cost-effective alternatives for applications requiring moderate accuracy.

Keywords: time transfer, GNSS, low-cost, clock comparison, Ublox F9T.

1. Introduction

In this article, we explore low-cost Global Navigation Satellite System (GNSS) receivers for time transfer applications. GNSS have had a profound impact on modern society by enabling precise positioning, navigation, and timing solutions. In particular, the accurate dissemination of time has become essential for numerous applications, ranging from telecommunications and financial transactions to scientific research and infrastructure management [1]. The use of GNSS signals for precise time transfer has evolved over the years, driven by advancements in receiver technology, methodologies, and processing algorithms that make the once cutting-edge technology available today in a low-cost package.

As technology has advanced, the capabilities of receivers have also changed. GNSS devices have evolved from single-channel to multi-channel geodetic and even timing receivers designed exclusively for time transfer. The concepts and requirements of devices for timing applications are described in [2]. Early implementations embraced the Common-View technique [3], where time synchronization was achieved by comparing measurements from separate receivers observing the same satellites according on a strict schedule. This approach evolved into the All-In-View method [4], where it is no longer necessary to observe the same satellite at the same time. A leap came with the emergence of Precise Point Positioning (PPP) ([5], [6], [7], [8]), which allowed a single receiver to simultaneously estimate its position and time by using precise satellite orbit and clock information to within a few millimeters.

Recent efforts in the field have proven that low-cost GNSS systems for time transfer can be developed. Institutions such as the National Institute of Standards and Technology (NIST) or the National Measurement Institute Australia have successfully implemented devices based on low-cost GNSS receivers [9], [10]. OpenTTP [11], an open-source initiative, is a testament to collaborative innovation in this domain and facilitates the collective development of low-cost GNSS receiver solutions.

2. Subject & methods

Three GNSS receivers were used in the experiment: the Trimble NetRS served as the reference receiver, while the Ublox RCB-F9T and M8T timing modules acted as Devices Under Test (DUT). All three receivers used the same Trimble Zephyr dual-frequency geodetic antenna and were compared to a 5071A cesium atomic clock (*CsIII*). Each receiver was capable of collecting raw measurement data for subsequent post-processing. The acquired measurements were then compared to those of the reference receiver and the differences were analyzed.

A. Measurement setup

The *CsIII* clock was connected to the external frequency input of the Trimble NetRS L1, L2 GPS receiver. This allows a direct comparision of the clock, which is located outside the receiver, with the GPS time. The raw receiver measurements were post-processed by the Canadian Spatial Reference Sys-

DOI: 10.2478/msr-2024-0006

*Corresponding author: marek.dorsic@gmail.com (M. Doršic)

tem Precise Point Positioning (CSRS-PPP) service, which is operated by the Geodetic Survey of National Resources Canada. Rapid orbits were used in the post-processing process and the algorithm incorporates the ambiguity resolution using phase and code measurements [12]. The CSRS-PPP clock solution plots the offset of the *CsIII* clock to GPS time within the observed period.

The Allan deviation [13] of the *CsIII* clock used, as determined by the reference, receiver was calculated. It renders bellow the specification limit of the 5071A clock (see to Fig. 1), which verifies the setup of the reference receiver.

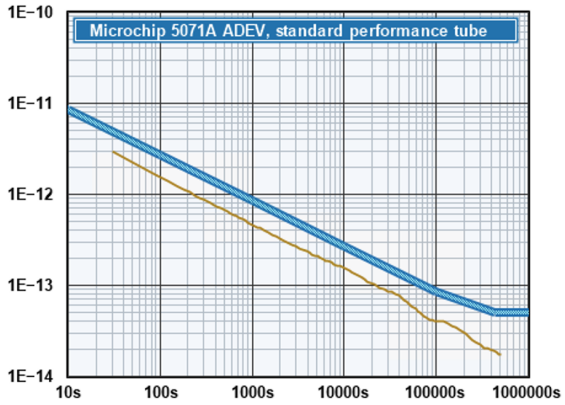

Fig. 1. Allan deviation $\sigma_y(\tau)$ of the *CsIII* atomic clock compared to GPS time with Trimble NetRS.

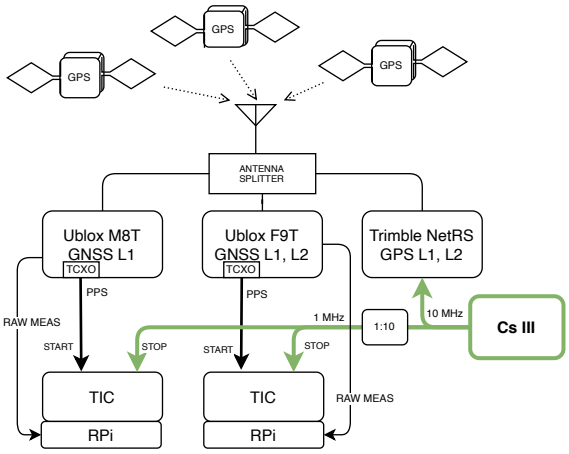

Fig. 2. The design of zero-baseline measurement.

The Pulse Per Second (PPS) signals of the Ublox timing modules were compared with the *CsIII* clock using time interval counters (see Fig. 2). An SR620 [14] counter compared the Ublox RCB-F9T module with *CsIII* and HP 53131 [15] compared with the Ublox M8T receiver. Both the Ublox timing modules use a local Temperature-compensated Crystal Oscillator (TXCO) to generate the pulses. The internal microprocessor unit takes care of using the closest edge of the TXCO and calculating the quantization error correction, also known as saw correction, which refers to the shape of the data (see Fig. 3).

The Ublox F9T chip incorporates an L1, L2 GNSS receiver, while the M8T is only a single-frequency receiver. The Ublox F9T can therefore measure and remove the first-order ionospheric correction by comparing the satellite signal transmitted at two different frequencies [16]. Single-frequency devices generally use the Klobuchar model [17], [16] to estimate of the signal propagation delay in the ionosphere with coefficients broadcasted in the navigation message, which is generally less effective than a direct measurement. The GPS, Galileo and Beidou constellations were enabled, the GPS timescale set for generating the PPS and fix position was set up in both receivers.

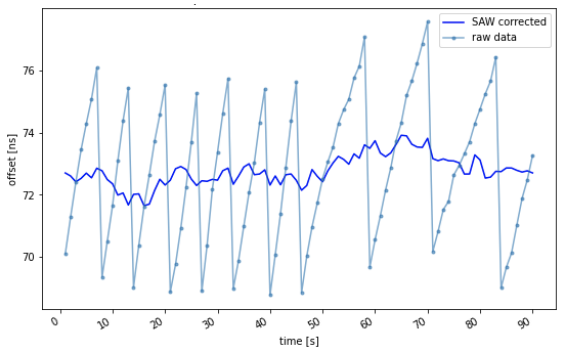

Fig. 3. The effect of quantization error (or saw) correction, Ublox RCB-F9T. Raw data from time interval counter is in light blue trace, dark blue trace is data after quantization error correction.

By using the same antenna for all receivers, thus establishing a zero-length baseline, atmospheric and antenna position biases are eliminated from the results. These biases represent significant error contributors in GNSS measurement processing. The antenna position was fixed to coordinates derived from the post-processed solution computed by the CSRS-PPP service, following an initial 24-hour survey campaign. The observation results are presented in Table 1. The estimated coordinates differ by ~5 cm when only then GPS constellation was used.

B. Observations processing

The measurements from the reference receiver were processed using the CSRS-PPP service in batches of 7 days each. These processed batches were subsequently trimmed, culminating in a final 20-day campaign. Each batch overlapped by one day with both the preceding and succeeding batches (see Fig. 4), so that discontinuities between batches could be removed [18].

For the raw data collected from the Ublox receivers, specific attention was paid to the reported PPS quantization error correction (see Fig. 3) and locked time for each epoch. The quantization error correction was used to offset the time interval counter readings. The reported locked time helped to detect local clock resets and to remove potential steps in the data series.

Table 1. Antenna positions as determined by the receivers and CSRS-PPP postprocessing using rapid orbits, where d_x, d_y, d_z, d_{height} represent absolute value differences in x, y, z coordinates and *height*, respectively, from the coordinates determined by the NetRS reference receiver.

Receiver	NetRS (ref)	Ublox F9T	Ublox M8T	Ublox F9T
Constellation	GPS	GPS	GPS	GPS, Glonass
$ECEFx$	4074804.806 m	4074804.837 m	4074804.690 m	4074804.812 m
$ECEFy$	1249242.816 m	1249242.826 m	1249242.833 m	1249242.819 m
$ECEFz$	4729556.463 m	4729556.500 m	4729556.260 m	4729556.468 m
$2 \cdot \sigma_x$	0.012 m	0.008 m	0.541 m	0.006 m
$2 \cdot \sigma_y$	0.010 m	0.004 m	0.541 m	0.003 m
$2 \cdot \sigma_z$	0.012 m	0.009 m	0.472 m	0.006 m
d_x		0.031 m	0.116 m	0.006 m
d_y		0.010 m	0.017 m	0.003 m
d_z		0.037 m	0.203 m	0.005 m
$\lvert\mathbf{d}\rvert$		0.049 m	0.234 m	0.009 m
lat	48.16798338 °	48.16798339 °	48.16798287 °	48.16798337 °
lon	17.04435273 °	17.04435273 °	17.04435341 °	17.04435275 °
height	271.384 m	271.433 m	271.162 m	271.392 m
d_{height}		0.049 m	0.222 m	0.008 m

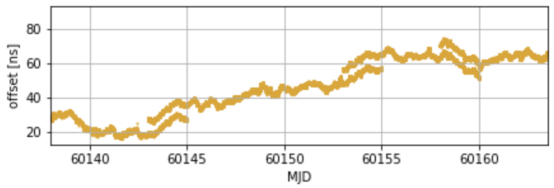

Fig. 4. CSRS-PPP processing batch discontinuities of the *CsIII* clock measured by the Trimble NetRS reference receiver.

C. *Receiver suitability assessment*

The clock solution of the reference receiver signifies the time difference between the *CsIII* atomic clock t_{clk} and the GPS timescale $t_{GPS(ref)}$ as realized by the reference receiver, expressed as

$$t_{clk} - t_{GPS(ref)} \tag{1}$$

The PPS of DUT embodies the realization of the GPS timescale by the receiver $t_{GPS(DUT)}$, whereby the counter readings representing the difference

$$t_{clk} - t_{GPS(DUT)} \tag{2}$$

By substracting (2) from (1) we obtain

$$t_{GPS(DUT)} - t_{GPS(ref)} = \varepsilon \tag{3}$$

The goal is to study the ε, which should be as small as possible to resemble the instabilities and viariantions of the local clock solutions, the PPS signal, the time interval measurement, and other errors. We neglected the constant systematic delays by aligning the overall mean values of the data series.

The time offsets of the *CsIII* clock from the GPS time, measured by the time interval counters at the receivers, are shown in Fig. 5. Notably, the Ublox F9T data series was offset by -5 ns for better visibility. The results of the dual-frequency receivers are well aligned with much less noise compared to the single-frequency M8T receiver. The Ublox M8T single-frequency receiver performed significantly worse, and showed large swings mainly because of its inability to directly measure the ionospheric delay and can only compensate for this to a limited extent using broadcasted parameters in the navigation message. This becomes even more evident when the residuals are formed as differences between the clock estimates of the DUT and the clock estimates of the reference receiver, as shown in Fig. 6.

The spread of the Ublox RCB-F9T residuals represents the difference between a solution with only real-time information available and PPP post-processed measurements of the reference receiver using more precise orbit and clock products.

From the time domain perspective, the Time Deviation (TDEV) [19] is more of greater interest. This only confirms that the data averaging of >200 s removes all quantization error (Fig. 7). The TDEV of the dual-frequency receiver remained well bellow 1 ns, dropping to only 0.3 ns at τ of 1 day.

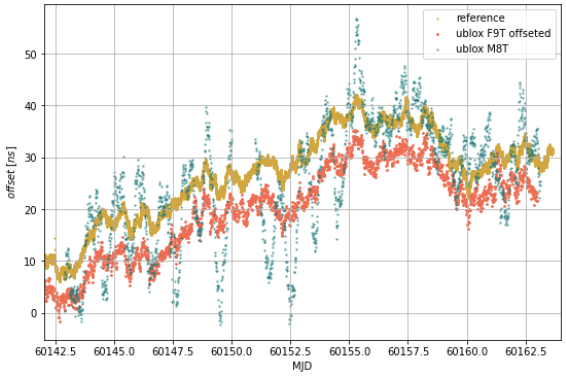

Fig. 5. Time offset of the *CsIII* clock from the GPS time as measured by different receivers. Yellow trace is the reference Trimble NetRS receiver, blue trace is the Ublox M8T receiver and red trace is the Ublox RCB-F9T receiver. Note the red trace was offset by -5 ns.

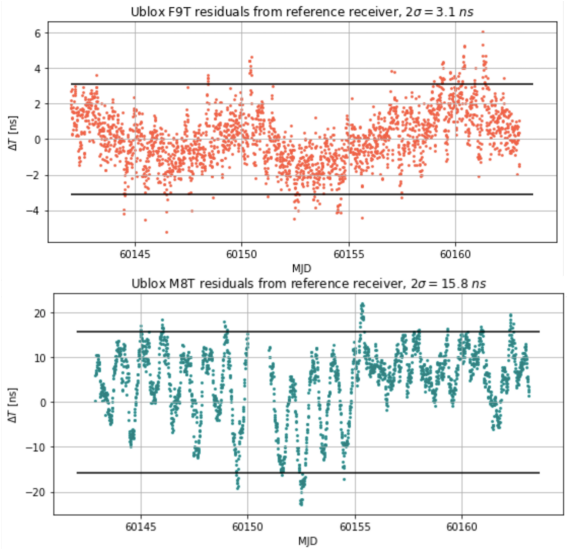

Fig. 6. Ublox F9T (top/red) and M8T (bottom/green) residuals from the reference receiver of saw corrected consecutive 780-second block averages. Bold black lines delineate $\pm 2\sigma$ interval.

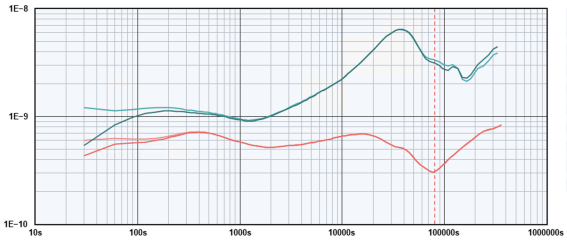

Fig. 7. Time deviation $\sigma_X(\tau)$ of the residuals for the Ublox M8T receiver, with light green trace representing raw data and dark green indicating saw-corrected data. The red traces stand for the Ublox F9T receiver, with light red representing raw data and dark red indicating saw-corrected data. The red vertical dotted line marks $\tau = 80000\ s$ or ~1 day.

In the frequency domain, the comparision of the dual-frequency receiver against the reference clock has a noise floor of 3.5×10^{-14} at $\tau = 1$ day, as can be seen from the Allan deviation results in Fig. 8.

3. Results

The study focused on evaluating the instability of clock comparison measurement using GNSS receivers in a zero-length baseline configuration. In particular, the Ublox F9T dual-frequency GNSS timing module exhibited 0.3 ns instability over a one-day averaging interval. In contrast, the Ublox M8T single-frequency GNSS timing module showed an order of magnitude worse performance with an instability of 3.3 ns at a $\tau = 1$ day. This disparity in performance emphasizes the importance of choosing the right GNSS receiver for applications that require high precision. It is noteworthy that single-frequency devices are used with a TDEV of less than 1 ns at $\tau = 1$ day are used at NIST [9].

The 780-second consecutive block averaging approach proved to be effective in minimizing the influence of quantization error, which can be averaged out. Consequently, the research suggests that without seeking to further post-process the raw measurements, data logging of the quantization error and processing has limited impact on long-term instability, and provides little improvement and both of the receivers perform at the expected specification level. This allows a significant reduction in system complexity, provided sufficiently long averaging intervals are used. However, for more precise applications and if standard CGGTTS files [20] are to be created for time comparision, raw data measurements and postprocessing are required.

4. Conclusions

Our investigation has provided insights into practical limitations and performance characteristics of low-cost GNSS receivers. Low-cost GNSS receivers, while cost-effective and accessible, are generally ill-suited for demanding high-precision time and frequency comparisons due to several inherent limitations. One limitation is the lack of external clock and frequency input, which affects their ability to provide accurate and stable measurements. The raw GNSS signal measurements primarily reflect the characteristics of their local oscillator rather than those of DUT, and the PPS output derived from the local oscillator must be compared with a time interval counter, which introduces uncertainties.

However, the study has highlighted the advantages of dual-frequency receivers. These receivers benefit from advanced signal processing and the ability to directly measure ionospheric corrections, resulting in up to an order of magnitude better results compared to their single-frequency counterparts, making them more suitable for high-precision applications.

Our experiment was limited to receivers from a single manufacturer. Other receivers, particularly single-frequency ones, may have different performance characteristics, ranging from

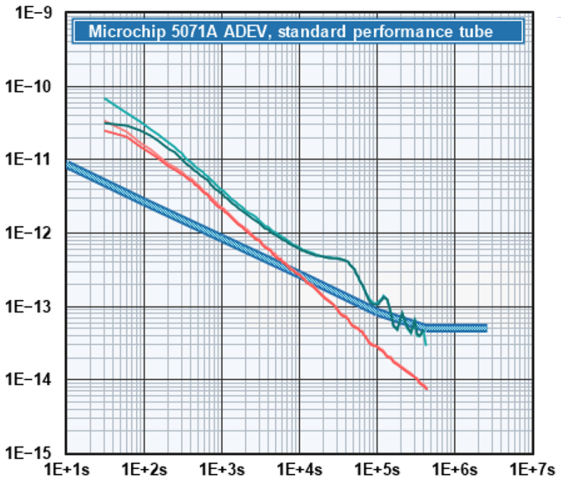

Fig. 8. Allan deviation plot of the receivers' residuals. The green traces represent the Ublox M8T receiver, with light green indicating raw data and dark green signifying saw corrected data. The red traces represent for Ublox F9T receiver, with light red denoting raw data and dark red indicating saw corrected data.

better to worse. Nonetheless, our results highlight their potential utility in certain scenarios where moderate accuracy is required and where they may be an attractive and cost-effective choice.

Finally, it is important to note that harware delays were not considered in the study. For absolute time transfer applications, these delays must be accurately measured and added to the total uncertainty budget. The lower-bound uncertainty we have identified represents the best-case scenario. In cases where different antennas are used over longer distances, one should expect larger uncertainties. These findings provide valuable guidance for the use of low-cost GNSS receivers in time transfer applications and emphasize the need for careful consideration of the specific requirements and limitations of their intended use cases.

Future work will aim to improve the results by developing tools for modeling the external clock offset out from the receiver's internal oscillator PPS signal and time interval counter readings and post-processing of raw measurements with the ability to generate CGGTTS outputs.

REFERENCES

[1] Sherman, J., Arissian, L., Brown, R., Deutch, M., Donley, E., Gerginov, V., Levine, J., Nelson, G., Novick, A., Patla, B., Parker, T., Stuhl, B., Sutton, D., Yao, J., Yates, W., Zhang, V., Lombardi, M. (2021). *A Resilient Architecture for the Realization and Distribution of Coordinated Universal Time to Critical Infrastructure Systems in the United States: Methodologies and Recommendations from the National Institute of Standards and Technology (NIST)*. Technical Note 2187. https://doi.org/https://doi.org/10.6028/NIST.TN.2187.

[2] Defraigne, P., Petit, G., Uhrich, P., Aerts, W. (2010). Requirements on GNSS receivers from the perspective of timing applications. In *EFTF-2010 24th European Frequency and Time Forum*. IEEE. https://doi.org/10.1109/EFTF.2010.6533724.

[3] Allan, D. W., Weiss, M. A. (1980). Accurate time and frequency transfer during common-view of a GPS satellite. In *34th Annual Symposium on Frequency Control.* IEEE, 334–346. https://doi.org/10.1109/FREQ.1980.200424.

[4] Weiss, M., Petit, G., Jiang, Z. (2005). A comparison of GPS common-view time transfer to all-in-view. In *Proceedings of the 2005 IEEE International Frequency Control Symposium and Exposition.* IEEE. https://doi.org/10.1109/FREQ.2005.1573953.

[5] Zumberge, J., Heflin, M., Jefferson, D., Watkins, M., Webb, F. (1997). Precise point positioning for the efficient and robust analysis of GPS data from large networks. *Journal of Geophysical Research,* 102(B3), 5005–5017. https://doi.org/10.1029/96JB03860.

[6] Weiss, M., Fenton, P., Powers, E., Senior, K. (2004). Frequency transfer using precise point positioning. In *18th European Frequency and Time Forum (EFTF 2004).* IET, 623–629. https://doi.org/10.1049/cp:20040942.

[7] Petit, G., Jiang, Z. (2008). Precise point positioning for TAI computation. *International Journal of Navigation and Observation,* 2008, 562878. https://doi.org/10.1155/2008/562878.

[8] Kouba, J., Héroux, P. (2001). Precise point positioning using IGS orbit and clock products. *GPS Solutions,* 5, 12–28. https://doi.org/10.1007/PL00012883.

[9] Lombardi, M., Novick, A., Zhang, V. (2014). A low-cost time transfer receiver for contributions to coordinated universal time. *Journal of Research of the National Institute of Standards and Technology,* 119, 583–601. https://doi.org/10.6028/jres.119.024.

[10] Wouters, M., Marais, E. (2019). Using low-cost receivers for multi-GNSS time transfer. In *2019 Joint Conference of the IEEE International Frequency Control Symposium and European Frequency and Time Forum (EFTF/IFC).* IEEE. https://doi.org/10.1109/FCS.2019.8856054.

[11] Wouters, M., Marais, E. L., Gupta, A., bin Omar, A., Phoonthong, P. (2019). The open traceable time platform: Open source software and hardware for dissemination of traceable time and frequency. In *2019 Joint Conference of the IEEE International Frequency Control Symposium and European Frequency and Time Forum (EFTF/IFC).* IEEE. https://doi.org/10.1109/FCS.2019.8856026.

[12] Banville, S. (2020). *CSRS-PPP Version 3: Tutorial*.

[13] Allan, D. W. (1966). Statistics of atomic frequency standards. *Proceedings of the IEEE,* 54(2), 221–230. https://doi.org/10.1109/PROC.1966.4634.

[14] Stanford Research Systems (1999). *MODEL SR620 Universal Time Interval Counter*. Revision 2.2.

[15] Hewlett-Packard Company (1996). *HP 53131A/132A 225 MHz Universal Counter*.

[16] Navstar GPS Joint Program Office. *IS-GPS-200, NAVSTAR GPS Space Segment/Navigation User Interfaces*.

[17] Klobuchar, J. A. (1987). Ionospheric time-delay algorithm for single-frequency GPS users. *IEEE Transactions on Aerospace and Electronic Systems,* AES-23(3), 325–331. https://doi.org/10.1109/TAES.1987.310829.

[18] Defraigne, P., Bruyninx, C. (2007). On the link between GPS pseudorange noise and day-boundary discontinuities in geodetic time transfer solutions. *GPS Solutions,* 11, 239–249. https://doi.org/10.1007/s10291-007-0054-z.

[19] Riley, W. J. (2008). *Handbook of Frequency Stability Analysis*. National Institute of Standards and Technology, NIST Special Publication 1065.

[20] Defraigne, P., Petit, G. (2015). CGGTTS-Version 2E: An extended standard for GNSS Time Transfer. *Metrologia,* 52(6), G1. https://doi.org/10.1088/0026-1394/52/6/G1.

Received September 23, 2023.
Accepted January 16, 2024.